OPEN ACCESS

University of BRISTOL

Publisher's PDF, also known as Version of record

License (if available):
CC BY-NC

Link to published version (if available):
[10.1126/sciadv.1701230](#)

[Link to publication record in Explore Bristol Research](#)
PDF-document

University of Bristol - Explore Bristol Research
General rights

PHYSICS

Heralded quantum steering over a high-loss channel

Morgan M. Weston,[1] Sergei Slussarenko,[1] Helen M. Chrzanowski,[1,2] Sabine Wollmann,[1,3] Lynden K. Shalm,[4] Varun B. Verma,[4] Michael S. Allman,[4] Sae Woo Nam,[4] Geoff J. Pryde[1]*

Entanglement is the key resource for many long-range quantum information tasks, including secure communication and fundamental tests of quantum physics. These tasks require robust verification of shared entanglement, but performing it over long distances is presently technologically intractable because the loss through an optical fiber or free-space channel opens up a detection loophole. We design and experimentally demonstrate a scheme that verifies entanglement in the presence of at least 14.8 ± 0.1 dB of added loss, equivalent to approximately 80 km of telecommunication fiber. Our protocol relies on entanglement swapping to herald the presence of a photon after the lossy channel, enabling event-ready implementation of quantum steering. This result overcomes the key barrier in device-independent communication under realistic high-loss scenarios and in the realization of a quantum repeater.

INTRODUCTION

A reliable method to send quantum information—say, from Alice to Bob—over long distances is to teleport it, using an entanglement shared by the two remote parties (*1, 2*). This entanglement resource could alternatively be used for generating secure correlated randomness between Alice and Bob, efficiently completing shared computational tasks (*3*), or testing nonlocality and quantum mechanics in new regimes such as when the parties are in different relativistic reference frames (*4, 5*). All these applications reach their potential only when entanglement is distributed over a long distance. Photons are excellent carriers of the quantum information, being a quantum version of the optical encodings used in existing long-distance classical telephony and data networking. However, in the quantum regime, attenuation (photon loss) is very destructive because the noise added by this process corrupts the entanglement. Thus, the maximum length of a quantum communication channel is restricted by propagation loss and environmental contamination.

The most secure quantum communication approaches—device-independent protocols (*6–8*)—and the most robust tests of nonlocality and quantum mechanics require verification of entanglement with stringent conditions on the amount of tolerable loss. For example, complete entanglement verification, through a violation of a Bell inequality, has recently been performed with the three main loopholes (*9*) closed simultaneously (*10–12*). Though these results represent a significant advance, practical limitations remain in exploiting these tests in a realistic long-distance scenario. Inevitable losses through any fiber or free-space channel open the detection loophole (*13*) for standard photonic implementations, forbidding a robust test even when the postselected measurement correlations are strong enough to violate a Bell inequality.

Here, to overcome the effect of loss in quantum channels, we adopt an event-ready approach (*14*). The key idea is to record an additional heralding signal that indicates whether the quantum state under investigation was successfully shared between Alice and Bob, that is, whether the particles are ready to be used in the verification protocol. By conditioning the validity of the protocol trial on this heralding signal, failed distribution events are excluded beforehand from being used in the test. We use entanglement swapping (*15–17*) to realize an event-ready scheme, allowing us to perform entanglement verification, that is detection loophole-free, over lossy quantum communication channels. Our approach also represents a central element of a more complex quantum repeater architecture, which may be used to overcome loss in very large networks.

RESULTS

We use an alternative test of nonlocality, quantum steering (also called Einstein-Podolsky-Rosen steering). Steering is an asymmetric protocol where one party, Bob, trusts quantum mechanics to describe his own measurements, whereas no assumptions are made about Alice, the other, untrusted, party (*18, 19*). The test may be satisfied by using entanglement to steer the state of a distant quantum system by local measurements on its counterpart. The nonlocal correlation verified by loophole-free steering both guarantees shared entanglement (*19*) and may be configured, with certain conditions, to implement one-sided device-independent quantum key distribution (QKD) (*7*).

In quantum steering, Alice's task is to convince Bob that she can influence his quantum measurement outcome for any choice of measurement setting that Bob provides to her. The formal steering protocol is shown in Fig. 1A. Bob's choice of measurement setting, labeled k, is chosen from a predetermined set of n observables. Bob's kth measurement setting corresponds to the Pauli observable $\hat{\sigma}_k^B$ for $k \in \{1,..,n\}$. We make no assumptions about what Alice is doing and thus represent her results as $A_k \in \{-1, 1\}$. Steps 1 to 3, from Fig. 1A, are iterated to obtain the average correlations between Alice's and Bob's results, known as the steering parameter (*19*)

$$S_n \equiv \frac{1}{n} \sum_{k=1}^{n} \left\langle A_k \hat{\sigma}_k^B \right\rangle \qquad (1)$$

If S_n is larger than a certain bound C_n (*19*), then Alice has successfully demonstrated quantum steering. Correct timing of these events is necessary to close the locality loophole (*20*), and Bob must have truly

[1]Centre for Quantum Dynamics and Centre for Quantum Computation and Communication Technology, Griffith University, Brisbane, Queensland 4111, Australia. [2]Clarendon Laboratory, University of Oxford, Parks Road, Oxford OX1 3PU, UK. [3]Quantum Engineering Technology Labs, H. H. Wills Physics Laboratory and Department of Electrical and Electronic Engineering, University of Bristol, BS8 1FD, UK. [4]National Institute of Standards and Technology, 325 Broadway, Boulder, CO 80305, USA.
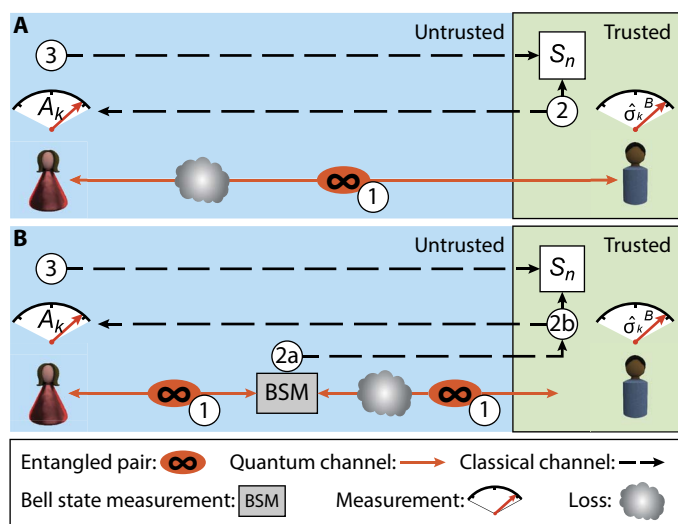*Corresponding author. Email: g.pryde@griffith.edu.au

Fig. 1. Conceptual representation of the quantum steering protocols. The blue background denotes untrusted channel components that belong to Alice, and the green background denotes the trusted side, Bob. (**A**) Conventional steering: ① Alice prepares a pair of photons and sends one of them to Bob. ② Bob announces his measurement setting, k, from a predetermined set of n observables. ③ Bob records his measurement outcome $\hat{\sigma}_k^B$, and Alice declares her result A_k. Steps 1 to 3 are iterated to obtain the steering parameter S_n. (**B**) Heralded quantum steering protocol. Bob uses a classical signal from a successful Bell state measurement (BSM) measurement ②a to herald the presence of Alice's photon after the lossy channel, ignoring all the trials when the BSM was not successful. From step ②b, the protocol proceeds as in (B).

Table 1. Experimental parameters and rates. The pump power P, approximate counting time, and total number of fourfold coincidence counts measured for different amounts of loss, L.

L (dB)	$P(PS_1)$ (mW)	$P(PS_2)$ (mW)	Count time (hours)	Fourfolds
7.7	100	50	8.3	730
11.3	90	40	21.6	549
14.8	75	40	98.5	594

random measurement choices to close the freedom-of-choice loophole. However, the focus of this work is on transmission loss.

A dishonest Alice—or an eavesdropper controlling Alice's apparatus—may attempt to use the fair sampling assumption (that is, an open detection loophole) to cheat by hiding incompatible measurement results (13). She may mimic perfect correlations of a maximally entangled state, and Bob has no way to determine whether a lack of measurement outcome announcement by Alice is due to genuine qubit loss or cheating. To prevent cheating, Bob requires Alice to announce her measurement result at least a certain fraction ε of trials, which we call Alice's heralding efficiency. When the entanglement verification is performed over long distances, the additional loss in Alice's channel will inevitably reduce the heralding efficiency below an acceptable value required for loophole-free entanglement verification.

The generalized steering bounds (21), which take into account Alice's heralding efficiency, allow detection loophole–free quantum steering in the presence of arbitrarily high loss in the untrusted quantum channel. However, guaranteed success for very high channel loss relies on the use of perfect pure entangled states and an infinite number of measurement settings, which is unrealistic in real-world scenarios.

Implementing an event-ready entanglement verification scheme allows us to herald the presence of the qubit in Alice's arm, increasing her effective heralding efficiency. In principle, this improved heralding could be realized in one of several ways, broadly including quantum nondemolition style measurements such as entanglement swapping (15–17), distillation techniques such as noiseless linear amplification (22, 23), and photonic qubit precertification (24). For the levels of loss considered here, we favor entanglement swapping, owing to its comparatively low resource overhead and high success rates. If entanglement

swapping is performed with spontaneous parametric downconversion (SPDC) sources, as here, then the squeezing parameter of those sources must be chosen carefully to control the effect of multiphoton events (see Table 1, Materials and Methods, and fig. S2).

The effective increase in heralding efficiency obtained with the entanglement swapping step allows us to avoid the detection loophole without assuming the honesty of Alice. Crucially, if the protocol is run in a fully time-ordered mode, as illustrated in fig. S1, Alice is forced to announce over a classical channel when the teleportation has been successful and thus declare which subset of measurement runs should be used to verify the entanglement before Bob announces his measurement settings. This prevents her from exploiting the nondeterminism of the swapping operation to introduce a loophole—announcing a false outcome of the entanglement swapping measurement gains her no advantage. Bob can then proceed with the steering verification protocol.

We performed our experiment using two polarization-entangled photon pairs generated by separate high–heralding efficiency sources (25), PS_1 and PS_2 (see Fig. 2 and Materials and Methods). The photon pairs were prepared in $|\Psi^-\rangle = (|HV\rangle - |VH\rangle)/\sqrt{2}$, where $|H\rangle$ and $|V\rangle$ denote horizontal and vertical polarizations, respectively. The signal photon from source PS_2 was sent to Bob for polarization analysis (B-PA) measurement, whereas the remaining photon from the same pair was sent through a variable-loss channel toward Alice.

In the first experiment, only source PS_2 was used, and Alice's channel contained no added loss. Alice directly received her photon from PS_2 into her polarization analyzer (A-PA)—no entanglement swapping was used. We performed the steering protocol with $n = 6$ measurement settings. Note that as the number of measurement settings is increased in steering protocols, the observation of steering is slightly more tolerant to loss (21), but with diminishing returns. At the same time, the deleterious effect of measurement-setting errors grows with increasing n. The choice of $n = 6$ provides a suitable balance between these effects. We observed detection loophole–free quantum steering with a steering parameter of $S_6 = 0.960 \pm 0.008$ and Alice's effective heralding efficiency of $\varepsilon = 0.4395 \pm 0.0003$, violating the C_n bound by 18 standard deviations (SDs).

In the second experiment, a variable channel loss L was added between the two parties by using a gradient ND filter (see Fig. 2). Using only source PS_2, we measured the steering parameter S_6 and Alice's effective heralding efficiency for various levels of added channel loss. The results are shown in Fig. 3C. With the addition of even 7.7 ± 0.1 dB of channel loss, the heralding efficiency dropped below the $C_\infty(\varepsilon)$ bound, forbidding secure quantum steering even in the limiting theoretical case of infinite measurement settings.

In the third experiment, we added source PS_1 and the entanglement swapping step, realized through a partial BSM, to herald Alice's photon (see Materials and Methods for details). An additional coincidence
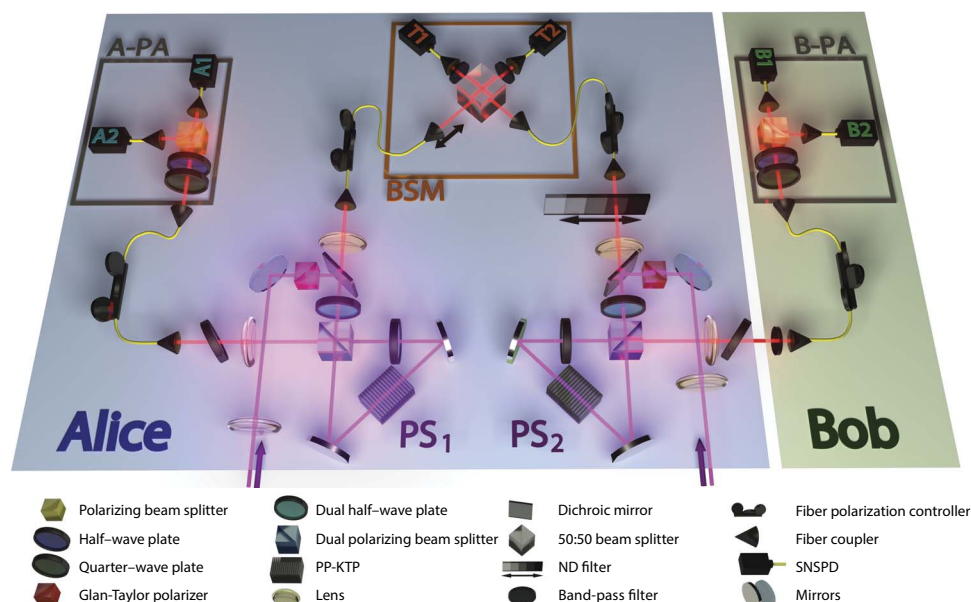
Fig. 2. Experimental setup. Two group-velocity-matched sources (*25*), PS$_1$ and PS$_2$, are pumped by a mode-locked femtosecond Ti:sapphire laser to generate two polarization-entangled photon pairs at 1570 nm in the $|\Psi^-\rangle$ state. Blue and green backgrounds outline the untrusted and trusted sides, respectively (all untrusted elements are grouped with Alice, even if they are not in her "lab" in practice). A-PA and B-PA are the polarization analyzer (tomography) stages of Alice and Bob, and BSM is the Bell state measurement gate, composed of a nonpolarizing 50:50 beam splitter. A variable neutral density (ND) filter is used in the output of PS$_2$ leading to the BSM to introduce the channel loss, *L*. Eight-nanometer band-pass (BP) filters were placed in the path of the photon going to B-PA and after beam splitter (BS), increasing the singlet state fidelity and interference visibility while maintaining Alice's high heralding efficiency. For the conventional steering measurement, the output of PS$_2$ containing the ND filter was directly connected to the A-PA stage through the fiber, bypassing the BSM gate and PS$_1$. SNSPD, superconducting nanowire single-photon detector; PP-KTP, periodically poled potassium titanyl phosphate.

detection signal from the two BSM detectors heralded a successful swapping operation. Alice's effective heralding efficiency at A-PA was then defined as the probability of detecting a four-photon coincidence from A-PA, B-PA, and the triggers at the BSM, given that a three-photon coincidence was detected from B-PA and triggers at the BSM. The final shared state ρ, with no added loss, was determined using quantum state tomography (*26*) and is shown in Fig. 3 (A and B). It had a singlet Bell state fidelity $F = \langle \Psi^- | \rho | \Psi^- \rangle = (91 \pm 3)\%$, which is comparable with the best value previously reported in entanglement swapping (*27*). Because PS$_1$ does not have unit heralding efficiency, the entanglement swapping does not produce deterministic arrival of a photon at Alice's polarization measurement. However, it increases this probability to a level compatible with demonstrating detection loophole–free steering: Her conditional heralding efficiency was recovered to ε ~ 0.45 (Fig. 3C).

Measured steering parameters of 0.874 ± 0.022, 0.862 ± 0.022, and 0.866 ± 0.024 and heralding efficiencies of 0.41 ± 0.02, 0.47 ± 0.02, and 0.43 ± 0.02, achieved in the presence of 7.7 ± 0.1, 11.3 ± 0.1, and 14.8 ± 0.1 dB of added loss, respectively, correspond to a successful violation of the $C_6(\varepsilon)$ bound by at least 2.2 SDs. A channel-added loss of 14.8 ± 0.1 dB is equivalent to 74 to 82 km of telecom optical fiber, assuming a fiber loss of 0.18 to 0.2 dB/km. It is worth noting that Alice's total channel loss, including the loss due to optical components in the BSM gate but excluding the detector efficiency, amounts to 20.0 ± 0.1 dB, which is equivalent to at least 100 km of telecom fiber.

DISCUSSION
As seen from Fig. 3C, we have not observed any degradation in the measured steering parameter or heralding efficiency while increasing

the amount of channel loss. This result suggests that the protocol is not limited to the demonstrated 14.8 ± 0.1 dB of added (20.0 ± 0.1 dB in total) loss and that achieving heralded quantum steering with higher values of loss is possible. Although the protocol can theoretically hold for arbitrarily high loss, increasing the loss significantly reduces the count rates (Table 1). Increasing loss will eventually result in unrealistic count times and in spurious coincidence rates caused by dark and background counts becoming comparable to real coincident photon detections. The point (that is, degree of loss) at which this happens is highly dependent on details of detector performance; because this is an area of rapid development in the community, we think that it is inadvisable to provide a specific numerical estimate at this time. Because the main breakthrough of our work is closing the detection loophole over a high-loss channel, we did not implement a randomized choice of measurement settings and time order of detection events in any of the steering protocol experiments.

Our heralded quantum steering protocol is the first demonstration of detection loophole–free entanglement verification over a high-loss channel. The ability to keep the quantum steering detection loophole closed with total losses of at least 20 ± 0.1 dB, and potentially higher, opens many new possibilities for security in long-range transmission through an optical fiber, free space, or between Earth and a satellite. With additional assumptions, it has been previously shown how to make a measurement device–independent version of the steering protocol (*28*) and how to turn quantum steering into a one-sided device-independent QKD scheme (*7*). This result is a considerable step toward the implementation of secure quantum communication and represents a single step quantum relay, a crucial component for future quantum repeaters.
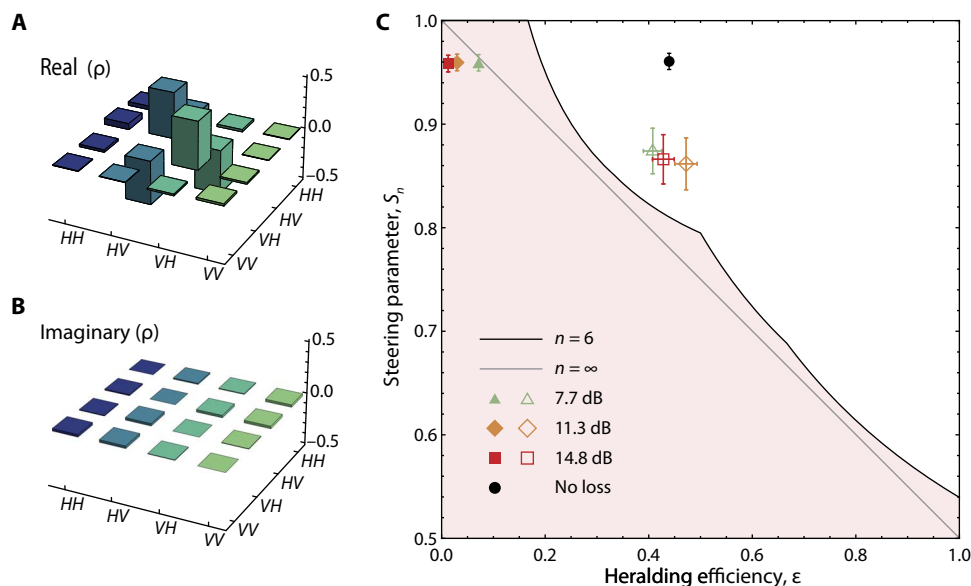
Fig. 3. Experimental results. (**A**) Real and (**B**) imaginary parts of the reconstructed density matrix ρ of the entanglement-swapped two-photon state with no additional loss applied to the quantum channel. (**C**) Quantum steering measurement results for different amounts of channel loss. Black and gray lines are, respectively, the $C_6(\varepsilon)$ and $C_\infty(\varepsilon)$ steering bounds from the study of Bennet *et al.* (*21*), and the red background highlights the region where detection loophole–free steering with the $n = 6$ measurement fails. The black circle, green triangles, yellow diamonds, and red squares mark the steering results achieved in the presence of 0, 7.7 ± 0.1, 11.3 ± 0.1, and 14.8 ± 0.1 dB of added channel loss, respectively. Filled markers correspond to steering parameters measured with the conventional steering protocol. Empty markers correspond to the heralded quantum steering results, each calculated from at least 500 fourfold coincidence counts (Table 1).

MATERIALS AND METHODS
Photon sources and characterization
The heralded quantum steering protocol relies on pure and indistinguishable entangled states. Conventional SPDC sources require narrowband [full width at half maximum (FWHM) < 2 nm] filters to erase the spectral distinguishability. These filters significantly decrease the heralding efficiency, making a detection loophole–free steering inequality violation impossible, unless other sources of noise and imperfection in the state are quite small, which is impractical for future practical application. To circumvent this obstacle, we developed a new type of SPDC photon source (*25*). Our sources work at the group velocity matching condition to generate frequency-uncorrelated photon pairs, removing the necessity of harsh spectral filtering.

We used two such polarization-entangled photon pair sources in the Sagnac interferometer configuration (PS$_1$ and PS$_2$ in Fig. 2), pumped by a mode-locked Ti:sapphire laser with an 81-MHz repetition rate, 785-nm wavelength, and 5.35-nm FWHM bandwidth. In each source, SPDC from a nonlinear periodically poled KTP crystal produced photon pairs with 1570-nm wavelength and ≈15-nm FWHM bandwidth. The Sagnac configuration provided polarization entanglement, whereas the pump and crystal parameters were selected to remove frequency correlations. The focusing and collection Gaussian beam modes were optimized to increase the heralding efficiency of the source, according to Weston *et al.* (*25*). Together with high-efficiency SNSPDs (*29*), we achieved heralding efficiencies of 0.47 ± 0.02 for each of our sources while maintaining the necessary high fidelity of entanglement swapping.

The entangled states produced by PS$_1$ and PS$_2$ were individually characterized via polarization state tomography. For each state, we used either A-PA or B-PA for one of the photon measurements. To measure the other photon in a pair, we inserted an additional polarization measurement stage in the BSM gate part of the setup (not shown in Fig. 2). The fidelity with the maximally entangled singlet Bell state, measured in

this way, was $F = (97.2 \pm 0.3)$ % for PS$_1$, where both photons were filtered with 8-nm BP filters, and $F = (98.2 \pm 0.3)$ % for PS$_2$, where the spectral filtering was applied only to the photon passing through the BSM part of the apparatus. Although the source needs very little spectral filtering to produce a high-fidelity state, this moderate filtering was used to overcome reductions in the fidelity caused by wavelength-dependent effects introduced by some optical components.

Entanglement swapping
The entanglement swapping works as follows. The photon Alice receives from PS$_2$ and one of the photons from PS$_1$ are input to a BSM gate, where they interfere nonclassically on a 50:50 nonpolarizing beam splitter (the remaining photon from PS$_1$ was sent to Alice's polarization analyzer). A coincidence detection signal from the two BSM detectors labels a successful projection onto the $|\Psi^-\rangle$ state, heralding a successful swapping operation. High-visibility Hong-Ou-Mandel (HOM) interference is required to perform the swapping operation with high fidelity. This was achieved while maintaining high entangled-state fidelity and high heralding efficiency, thanks to our high-performance sources (*25*) and high-efficiency, low-noise SNSPDs (*29*).

We measured HOM interference visibility in the BSM gate to characterize the indistinguishability of the photons from PS$_1$ and PS$_2$. One photon from each maximally entangled pair was sent to BSM, whereas the remaining photons of each pair were sent to A-PA and B-PA and projected into the $\{|H\rangle, |V\rangle\}$ basis. We used 8-nm BP filters at the output of the BSM stage to maximize interference visibility and on the heralding photon of the PS$_2$ photon pair. No polarization optics were used inside the BSM gate. We observed visibilities of (90 ± 3) % for $|V\rangle$ polarized photons and (99 ± 4) % for $|H\rangle$ polarized photons. We attribute the lower visibility value to the residual polarization distinguishability of interfering photons, arising from the nonsymmetric (47:53) splitting ratio of our BS for vertical polarization and,

more significantly, from the lack of spectral flatness of optical coatings of optical components over the wide frequency band of our photons.

Channel loss

Alice's added channel loss, L, was implemented by using two variable ND filters, whose transmission was characterized separately using a 1570-nm diode laser. Eight-nanometer BP filters introduced an additional 3.5 ± 0.1 dB of loss, and the loss due to optical components and fiber coupling of the BSM gate was measured to be 1.7 ± 0.1 dB. Together with $L = 14.8 \pm 0.1$ dB of maximum added loss, the highest total loss applied to the channel was 20 ± 0.1 dB, excluding the nonunit quantum efficiency of the SNSPDs.

High-order SPDC pair generation

The pumping powers $P(PS_1)$ and $P(PS_2)$ of our sources were kept below 100 mW to keep the impact of high-order pair production on the independent HOM interference and state quality negligible (*25, 30*). In the presence of added loss, the fractional contribution of high-order terms from PS_1 increases. However, the probability of generating a photon pair from each source is comparable with the probability of generating two photon pairs from PS_2. The latter events produce false heralding coincidences, significantly decreasing Alice's heralding efficiency (see fig. S2). Efficient heralding of entanglement swapping requires that the number of photons from one side (for example, source PS_2) is significantly lower than the number of photons from the other side (source PS_1). With the increased channel loss, this condition is satisfied automatically even for the equal raw brightness of PS_1 and PS_2. Nevertheless, careful selection of appropriate pump powers for these sources is still required. We found that as the loss was increased, $P(PS_1)$ had to be decreased to keep the swapped-state quality high, and $P(PS_2)$ had to be matched accordingly to maintain the heralding efficiency. The pump powers chosen for different levels of added loss are shown in Table 1.

Experimental uncertainties

The measurement uncertainties for the quantum steering parameters comprise heralding efficiency uncertainty and steering parameter uncertainty, denoted by horizontal and vertical error bars, respectively, in Fig. 3C. The latter takes into account both systematic measurement error and Poissonian photon counting noise. The systematic error contribution occurs because of the imperfections in optical components of Bob's measurement apparatus, which could result in an overestimate of the steering parameter. We used the systematic error estimation procedure developed by Bennet *et al.* (*21*). This procedure assumes a perfect entangled state and attributes any deviation from $S_n = 1$ to the imperfection of Bob's measurement apparatus. Such an approach overestimates the steering parameter systematic uncertainty, when applied to our experimental data, where $S_n < 1$ is known to arise predominantly from imperfect entangled states and imperfect entanglement swapping. The uncertainties in state parameters derived from quantum state tomography were calculated through standard error propagation techniques applied to a distribution of reconstructed density matrices arising from a Monte Carlo calculation, which samples from Poissonian distributions of photon counts.

SUPPLEMENTARY MATERIALS

Supplementary material for this article is available at http://advances.sciencemag.org/cgi/content/full/4/1/e1701230/DC1

fig. S1. Proposed space-time diagram of the heralded steering protocol, illustrating the conditions to close the locality and freedom-of-choice loopholes.
fig. S2. Alice's heralding efficiency.

REFERENCES AND NOTES

1. M. Nielsen, I. Chuang, *Quantum Computation and Quantum Information. Cambridge Series on Information and the Natural Sciences* (Cambridge Univ. Press, 2000).
2. R. Horodecki, P. Horodecki, M. Horodecki, K. Horodecki, Quantum entanglement. *Rev. Mod. Phys.* **81**, 865–942, (2009).
3. T. C. Ralph, G. J. Pryde, Optical quantum computation. *Prog. Opt.* **54**, 209–269 (2009).
4. D. Rideout, T. Jennewein, G. Amelino-Camelia, T. F. Demarie, B. L. Higgins, A. Kempf, A. Kent, R. Laflamme, X. Ma, R. B. Mann, E. Martín-Martínez, N. C. Menicucci, J. Moffat, C. Simon, R. Sorkin, L. Smolin, D. R. Terno, Fundamental quantum optics experiments conceivable with satellites—Reaching relativistic distances and velocities. *Class. Quant. Grav.* **29**, 224011 (2012).
5. P. M. Alsing, I. Fuentes, Observer-dependent entanglement. *Class. Quant. Grav.* **29**, 224001 (2012).
6. A. Acín, N. Gisin, L. Masanes, From Bell's theorem to secure quantum key distribution. *Phys. Rev. Lett.* **97**, 120405 (2006).
7. C. Branciard, E. G. Cavalcanti, S. P. Walborn, V. Scarani, H. M. Wiseman, One-sided device-independent quantum key distribution: Security, feasibility, and the connection with steering, *Phys. Rev. A* **85**, 010301 (2012).
8. L. C. Comandar, M. Lucamarini, B. Fröhlich, J. F. Dynes, A. W. Sharpe, S. W.-B. Tam, Z. L. Yuan, R. V. Penty, A. J. Shields, Quantum key distribution without detector vulnerabilities using optically seeded lasers. *Nat. Photonics* **10**, 312–315 (2016).
9. J.-Å. Larsson, Loopholes in Bell inequality tests of local realism. *J. Phys. A Math. Theor.* **47**, 424003 (2014).
10. L. K. Shalm, E. Meyer-Scott, B. G. Christensen, P. Bierhorst, M. A. Wayne, M. J. Stevens, T. Gerrits, S. Glancy, D. R. Hamel, M. S. Allman, K. J. Coakley, S. D. Dyer, C. Hodge, A. E. Lita, V. B. Verma, C. Lambrocco, E. Tortorici, A. L. Migdall, Y. Zhang, D. R. Kumor, W. H. Farr, F. Marsili, M. D. Shaw, J. A. Stern, C. Abellán, W. Amaya, V. Pruneri, T. Jennewein, M. W. Mitchell, P. G. Kwiat, J. C. Bienfang, R. P. Mirin, E. Knill, S. W. Nam, Strong loophole-free test of local realism. *Phys. Rev. Lett.* **115**, 250402 (2015).
11. M. Giustina, M. A. M. Versteegh, S. Wengerowsky, J. Handsteiner, A. Hochrainer, K. Phelan, F. Steinlechner, J. Kofler, J.-Å. Larsson, C. Abellán, W. Amaya, V. Pruneri, M. W. Mitchell, J. Beyer, T. Gerrits, A. E. Lita, L. K. Shalm, S. W. Nam, T. Scheidl, R. Ursin, B. Wittmann, A. Zeilinger, Significant-loophole-free test of Bell's theorem with entangled photons. *Phys. Rev. Lett.* **115**, 250401 (2015).
12. B. Hensen, H. Bernien, A. E. Dréau, A. Reiserer, N. Kalb, M. S. Blok, J. Ruitenberg, R. F. L. Vermeulen, R. N. Schouten, C. Abellán, W. Amaya, V. Pruneri, M. W. Mitchell, M. Markham, D. J. Twitchen, D. Elkouss, S. Wehner, T. H. Taminiau, R. Hanson, Loophole-free Bell inequality violation using electron spins separated by 1.3 kilometres. *Nature* **526**, 682–686 (2015).
13. P. M. Pearle, Hidden-variable example based upon data rejection. *Phys. Rev. D* **2**, 1418–1425 (1970).
14. M. Żukowski, A. Zeilinger, M. A. Horne, A. K. Ekert, "Event-ready-detectors" Bell experiment via entanglement swapping. *Phys. Rev. Lett.* **71**, 4287–4290 (1993).
15. J.-W. Pan, D. Bouwmeester, H. Weinfurter, A. Zeilinger, Experimental entanglement swapping: Entangling photons that never interacted. *Phys. Rev. Lett.* **80**, 3891–3894 (1998).
16. R. Kaltenbaek, R. Prevedel, M. Aspelmeyer, A. Zeilinger, High-fidelity entanglement swapping with fully independent sources. *Phys. Rev. A* **79**, 040302(R) (2009).
17. R.-B. Jin, M. Takeoka, U. Takagi, R. Shimizu, M. Sasaki, Highly efficient entanglement swapping and teleportation at telecom wavelength. *Sci. Rep.* **5**, 9333 (2015).
18. H. M. Wiseman, S. J. Jones, A. C. Doherty, Steering, entanglement, nonlocality, and the Einstein-Podolsky-Rosen paradox. *Phys. Rev. Lett.* **98**, 140402 (2007).
19. D. J. Saunders, S. J. Jones, H. M. Wiseman, G. J. Pryde, Experimental EPR-steering using Bell-local states. *Nat. Phys.* **6**, 845–849 (2010).
20. B. Wittmann, S. Ramelow, F. Steinlechner, N. K. Langford, N. Brunner, H. M. Wiseman, R. Ursin, A. Zeilinger, Loophole-free Einstein-Podolsky-Rosen experiment via quantum steering. *New J. Phys.* **14**, 053030 (2012).
21. A. J. Bennet, D. A. Evans, D. J. Saunders, C. Branciard, E. G. Cavalcanti, H. M. Wiseman, G. J. Pryde, Arbitrarily loss-tolerant Einstein-Podolsky-Rosen steering allowing a demonstration over 1 km of optical fiber with no detection loophole. *Phys. Rev. X* **2**, 031003 (2012).
22. S. Kocsis, G. Y. Xiang, T. C. Ralph, G. J. Pryde, Heralded noiseless amplification of a photon polarization qubit. *Nat. Phys.* **9**, 23–28 (2013).
23. A. E. Ulanov, I. A. Fedorov, A. A. Pushkina, Y. V. Kurochkin, T. C. Ralph, A. I. Lvovsky, Undoing the effect of loss on quantum entanglement. *Nat. Photonics* **9**, 764–768 (2015).

24. E. Meyer-Scott, D. McCloskey, K. Gołos, J. Z. Salvail, K. A. G. Fisher, D. R. Hamel, A. Cabello, K. J. Resch, T. Jennewein, Certifying the presence of a photonic qubit by splitting it in two. *Phys. Rev. Lett.* **116**, 070501 (2016).

25. M. M. Weston, H. M. Chrzanowski, S. Wollmann, A. Boston, J. Ho, L. K. Shalm, V. B. Verma, M. S. Allman, S. W. Nam, R. B. Patel, S. Slussarenko, G. J. Pryde. Efficient and pure femtosecond-pulse-length source of polarization-entangled photons. *Opt. Express* **24**, 10869–10879 (2016).

26. A. G. White, A. Gilchrist, G. J. Pryde, J. L. O'Brien, M. J. Bremner, N. K. Langford, Measuring two-qubit gates. *J. Opt. Soc. Am. B* **24**, 172–183 (2007).

27. Q.-L. Wu, N. Namekata, S. Inoue, High-fidelity entanglement swapping at telecommunication wavelengths. *J. Phys. B* **46**, 235503 (2013).

28. S. Kocsis, M. J. W. Hall, A. J. Bennet, D. J. Saunders, G. J. Pryde, Experimental measurement-device-independent verification of quantum steering. *Nat. Commun.* **6**, 5886 (2015).

29. F. Marsili, V. B. Verma, J. A. Stern, S. Harrington, A. E. Lita, T. Gerrits, I. Vayshenker, B. Baek, M. D. Shaw, R. P. Mirin, S. W. Nam, Detecting single infrared photons with 93% system efficiency. *Nat. Photonics* **7**, 210–214 (2013).

30. J. Fulconis, O. Alibart, W. J. Wadsworth, J. G. Rarity, Quantum interference with photon pairs using two micro-structured fibres. *New J. Phys.* **9**, 276 (2007).

ScienceAdvances

Heralded quantum steering over a high-loss channel

Morgan M. Weston, Sergei Slussarenko, Helen M. Chrzanowski, Sabine Wollmann, Lynden K. Shalm, Varun B. Verma, Michael S. Allman, Sae Woo Nam and Geoff J. Pryde

ARTICLE TOOLS	http://advances.sciencemag.org/content/4/1/e1701230
SUPPLEMENTARY MATERIALS	http://advances.sciencemag.org/content/suppl/2017/12/22/4.1.e1701230.DC1
REFERENCES	This article cites 29 articles, 0 of which you can access for free http://advances.sciencemag.org/content/4/1/e1701230#BIBL
PERMISSIONS	http://www.sciencemag.org/help/reprints-and-permissions

Use of this article is subject to the Terms of Service